Conformational Preferences and Pathways for Enantiomerization and Diastereomerization of Benzyl Alcohol. Data Mining and ab Initio Quantum-Mechanical Study

Rainer Glaser* and G. Richard Nichols

Department of Chemistry, University of Missouri—Columbia, Columbia, Missouri 65211

Received September 9, 1999

The potential energy surface of benzyl alcohol has been explored at the RHF/6-31G* and MP2-(full)/6-31G* levels of ab initio theory. The exo and endo minimum structures and all of the transition-state structures for their enantiomerization and diastereomerization were located. The thermochemical functions were computed, and relative enthalpies and free enthalpies were determined. The computed relative free enthalpy is in excellent agreement with known NMR data. Benzyl alcohol is a highly flexible molecule, which allows for essentially unhindered enantiomerization and diastereomerization of the minima; all pertinent relative energies and free enthalpies are less than 3 kcal/mol, and the entire conformational space about the CC and CO bonds is easily accessible. An examination of the crystallographic record shows a much greater variety of conformations to occur in the solid state as a result of the optimization of intermolecular interactions in the crystals. Data mining shows that the conformations about the CC and CO bonds of all of the CC-staggered and CO-gauche structures are correlated, and consequently, the conformational preferences about the C−O bond greatly deviate from the expected 3-fold barrier. The theoretical study shows the correlation to be instrinsic and offers an explanation. Natural population analysis provides a rational for the relative stabilities of the benzyl alcohol conformations on the basis of the conformation dependence of the effects of electron−electron repulsion between the O-lone pairs and the benzene π-cloud, the charge−charge attraction between the hydroxyl H-atom and the benzene π-density, and the dipole−dipole interaction associated with the CH_2-C_{ipso} and OH bonds. Our analysis emphasizes the importance of the dipole alignment of the CH_2-C_{ipso} and OH bond dipole moments.

Introduction

Diazonium ions[1] are thought to play a crucial role in chemical carcinogenesis. A variety of amine derivatives are transformed into alkyldiazohydroxides, and heterolysis leads in many cases to diazonium ions[2] as the primary alkylating reagents. In particular, the decompositions of benzyl systems (R = Ph) continues to be a matter of debate.[3−8] We have recently reported the results of an ab initio study of "benzyldiazonium ion" in which we have shown that the interaction of N_2 with benzyl cation results in an electrostatically bound complex with a long C−N distance as the most stable structure.[9] We are now studying nucleophilic substitutions of benzyldiazonium ion and of its derivatives $PhCH_2N{=}NX$ (X = OH, OR, NH_2, etc.). Benzyl alcohol is formed in these reactions, and we needed to learn about its structure and properties. The exploration of the potential energy surface of benzyl alcohol turned out more interesting than anticipated. There is surprisingly little known about the stereochemistry of alkylbenzenes,[10] and a lack of theoretical calculations of benzyl alcohol has recently been pointed out.[11] Benzyl alcohol has been studied extensively by IR spectroscopy, and in CCl_4, CS_2, and DMSO solutions the IR spectrum clearly reveals the presence of two conformations.[12] More than 25 years ago, Pople et al.[13] studied several conformations of benzyl alcohol at the RHF/STO-3G level and using standard structural parameters. Three C_s structures were found to be nearly isoenergetic, within less than 0.25 kcal/mol, and these structures included the CC-eclipsed and CO-trans structure and the exo and endo structures with the CC-perpendicular conformation. A few years later, Abraham and Bakke[14] studied the conformations of benzyl alcohol

* To whom correspondence should be addressed. Phone: (573) 882-0331. E-mail: GlaserR@missouri.edu.

(1) For comprehensive recent reviews of diazonium ion chemistry, see: Zollinger, H. *Diazo Chemistry I* and *Diazo Chemistry II*, VCH: Weinheim, Germany, 1994 and 1995, respectively.

(2) (a) Hovinen, J.; Fishbein, J. *J. Am. Chem. Soc.* **1992**, *114*, 366. (b) Hovinen, J.; Finneman, J. I.; Satapathy, S. N.; Ho, J.; Fishbein, J. C. *J. Am. Chem. Soc.* **1992**, *114*, 10321. (c) Finneman, J. I.; Ho, J.; Fishbein, J. C. *J. Am. Chem. Soc.* **1993**, *115*, 3016. (d) Ho, J.; Fishbein, J. C. *J. Am. Chem. Soc.* **1994**, *116*, 6611.

(3) Capuano, L.; Dürr, H.; Zander, R. *Liebigs Ann. Chem.* **1969**, *721*, 75.

(4) Jugelt, W.; Berseck, L. *Tetrahedron* **1970**, 5581.

(5) (a) Dahn, H.; Diderich, G. *Helv. Chim. Acta* **1971**, *54*, 1950. (b) Diderich, G.; Dahn, H. *Helv. Chim. Acta.* **1972**, *55*, 1.

(6) Finneman, J. I.; Fishbein, J. C. *J. Am. Chem. Soc.* **1994**, *59*, 6251.

(7) (a) Finneman, J. I.; Fishbein, J. C. *J. Am. Chem. Soc.* **1995**, *117*, 4228. (b) Finneman, J. I.; Fishbein, J. C. *J. Am. Chem. Soc.* **1996**, *118*, 7134.

(8) White, E. H.; Field, K. W.; Hendrickson, W. H.; Dzadzic, P.; Roswell, D. F.; Paik, S.; Mullen, P. W. *J. Am. Chem. Soc.* **1992**, *114*, 8023 and references therein.

(9) Glaser, R.; Farmer, D. *Chem. Eur. J.* **1997**, *3*, 1244.

(10) For a discussion of the conformations of alkylbenzenes and related compounds, see: Eliel, E. L.; Wilen, S. H. *Stereochemistry of Organic Compounds*; John Wiley & Sons: New York, NY, 1994; p 625 ff.

(11) Gingell, J. M.; Marston, G.; Mason, N. J.; Zhao, H.; Siggel, M. R. F. *Chem. Phys.* **1998**, *237*, 443.

(12) Visser, T.; Van der Maas, J. H. *Spectrochim. Acta, Part A* **1986**, *42A*, 599 and references therein.

(13) Hehre, W. J.; Radom, L.; Pople, J. A. *J. Am. Chem. Soc.* **1972**, *94*, 1496.

(14) Abraham, R. J.; Bakke, J. M. *Tetrahedron* **1978**, *34*, 2947.

10.1021/jo991423q CCC: $19.00
Published on Web 01/07/2000

using NMR spectroscopy ($^3J(CH_2OH)$, $^2J(HCH)$, and chemical shift of OH) and their RHF/STO-3G energy calculations based on standard structures showed that "the endo conformation of the OH proton (anti to a C−H proton) is favored by approximately 1 kcal/mol over the *exo* conformation (H anti to Ph) and [that] these conformers are responsible for the two HO frequencies observed in the IR spectrum." The first potential energy surface analysis of benzyl alcohol was not performed until the late 1980s[15] when Schaefer et al. described a potential energy surface scan using a minimal basis set and keeping the geometry of the benzene ring fixed. This work suggested an endo structure with ∠(O−C−C−C) = 42.9° and ∠(H−O−C−C) = 60.2° as the most stable structure. An endo structure also is suggested by the electron diffraction study by Traetteberg et al.[16] This study shows that the O-atom is twisted out of the benzene plane with ∠(O−C−C−C) = 54° while the position of the hydroxyl H-atom could not be determined with certainty. The supersonic jet studies by Bernstein et al.[17] employed mass resolved excitation spectroscopy (MRES) to probe the conformations of a series of substituted benzyl alcohols. These studies found *one* minimum, and it was argued that its conformation most likely is perpendicular and endo with ∠(O−C−C−C) = 90° and ∠(H−O−C−C) = 0°, respectively. Most recently, Ebata et al.[18] reported the detection of *two* conformations of benzyl alcohol in a supersonic jet by way of IR−UV double-resonance spectroscopy. Neither of these minima was considered to have a perpendicular structure, and instead, on the basis of RHF/6-31G calculations, it was concluded that the more stable minimum was a CC-gauche and HO-endo structure and that the less stable conformation was the CC-eclipsed and HO-exo structure.

On this basis, a comprehensive study of the stereochemistry of benzyl alcohol is the issue of the present paper. We have explored the potential energy surface of benzyl alcohol locating not only the minima but also the transition-state structures for enantiomerization and diastereomerization. The potential energy surface analysis has been carried out at the Hartree−Fock level of ab initio theory and, importantly, also with the inclusion of electron correlation by way of second-order perturbation theory. All these computations employed the split-valence and polarized basis set 6-31G*. Furthermore, we have determined the thermochemical functions so that relative energies can be converted into relative enthalpies and free enthalpies. Benzyl alcohol presents two conformational issues. There are the questions as to the conformation about the C−C and C−O bonds. As far as the C−C conformation is concerned, one might consider the staggered conformations **I** and **II** and the eclipsed conformations **III** and **IV** (Scheme 1). With a view to the conformation of the C−O bond relative to the benzene plane, it suffices to consider types **I**−**III**.[19] We will refer to the

Scheme 1. Types of Possible CC Conformations

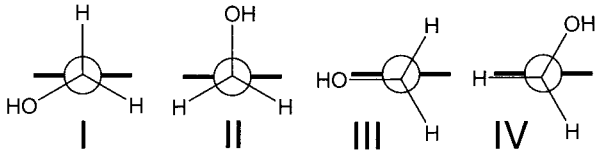

type **I** structures as the staggered structures and differentiate these from the type **II** structures by referrring to the latter as the staggered perpendicular structures. The descriptor "perpendicular" is meant to remind one that the C−O bond is perpendicular, or nearly so, with respect to the phenyl plane when viewed down the Ph−CH_2OH bond. We will refer structures of types **I**−**III** as structures **1**−**3** in the following, and letters **a**, **b**, **c** ... will be employed to indicate differences in the conformations about the O−C bond. An examination of the crystallographic record shows that a great variety of conformations occur in the solid state, and the data mining presents a first indication that the two main degrees of freedom are not independent. We will show that the conformations about the CC and CO bonds are correlated with each other and that conformational preferences about the C−O bond deviate from the expected 3-fold barrier. The results are explained on the basis of the conformation dependence of the effects of electron−electron repulsion between the O-lone pairs and the benzene π-cloud, the charge−charge attraction between the hydroxyl H-atom and the benzene π-density, and the dipole−dipole interaction associated with the CH_2-C_{ipso} and OH bonds.

Data Mining

The Cambridge Structural Database[20,21] was searched in two ways. First, we searched for structures that contained the parent benzyl alcohol itself. While the crystal structure of pure benzyl alcohol is not contained in the database, several crystal structures were determined that contained benzyl alcohol as a solvent molecule. These entries are collected on top of Table 1. Then we searched for benzyl alcohol derivatives constraining the search to molecules that contain the $-CH_2OH$ fragment. A large number of such molecules had been studied by X-ray crystallography, and summaries of their conformational properties are collected in Table 1. Database entries with questionable space groups were not considered.

For each entry in Table 1, we are providing the code name used in the database; full citations can be found in the database, and they are omitted here for brevity. Each benzyl alcohol moiety is characterized by the dihedral angles ∠(O−C−C−C) and ∠(H−O−C−C), which describe the conformations about the C−C and the C−O bonds. The positions of the alcohol H-atoms are given whenever they were reported. (There are several crystals that contain several independent benzyl alcohols for which the positions of some hydroxyl H-atoms have been

(15) Schaefer, T.; Sebastian, R.; Peeling, J.; Penner, G. H.; Koh, K. *Can. J. Chem.* **1989**, *67*, 1015.

(16) Traetteberg, M.; Oestensen, H.; Seip, R. *Acta Chim. Scand. A* **1980**, *A34*, 449.

(17) Im, H.-S.; Bernstein, E. R.; Secor, H. V.; Seeman, J. I. *J. Am. Chem. Soc.* **1991**, *113*, 4422.

(18) Guchhait, N.; Ebata, T. Mikami, N. *J. Am. Chem. Soc.* **1999**, *121*, 5705.

(19) **I** and **IV** can be viewed combined as "gauche," **II** as "perpendicular," and **III** as "eclipsed." Compare the discussion of ethylbenzene: Breen, P. J.; Bernstein, E. R.; Seeman, J. I. *J. Phys. Chem.* **1987**, *87*, 3269.

(20) (a) Cambridge Structural Database (CSD). Cambridge Crystallographic Data Centre, 12 Union Road. Cambridge, CB2 1EZ, U.K. (b) For details, see the home pages of the Cambridge Crystallographic Data Centre at URL http://www.ccdc.cam.ac.uk/index.html.

(21) Use of the structural databases for data mining and knowledge acquisition: (a) Allen, F. H. *Acta Crystallogr., Sect. A* **1998**, *A54*, 758. (b) Allen, F. H.; Pitchford, N. A. *NATO ASI Ser., Ser. E* **1998**, *352*, 15. (c) Allen, F. H.; Kennard, O. *Chem. Design Automation News* **1993**, *8*, 1 and 31.

Table 1. Conformational Properties of Reported Crystal Structures of Benzyl Alcohols

CSD record	∠(O−C−C−C)[a]	C−C type[b]	∠(H−O−C−C)	O−C type[c]	CSD record	∠(O−C−C−C)	C−C type	∠(H−O−C−C)	O−C type
				benzyl alcohol					
DEBGOG	18.6	staggered	112.5	cis, C−H	WIHCEV	24.0	staggered		
FAXLAR	8.3	eclipsed			WILJAC	67.6	stag. perp.		
JATNIB	10.0	eclipsed			YOVVAG	72.0	stag. perp.	175.0	trans
				BnOH derivatives					
BAGBAM	−76.0	stag. perp.	−163.4	trans	OHIBNZ	−14.5	eclipsed		
	−5.2	eclipsed	−144.0	cis, C−H	PAMJES	7.4	eclipsed		
BHHPHE	16.3	staggered	−171.6	trans	RAVREL	−7.9	eclipsed	−70.0	gauche
BZALPZ	−12.5	eclipsed	77.8	gauche		−66.8	stag. perp.	159.0	trans
	−80.2	stag. perp.	60.7	gauche	SALBUT	−87.8	stag. perp.		
CAGZIT	16.8	staggered	−161.9	trans		81.3	stag. perp.	43.0	gauche
CEBTIZ	65.4	stag. perp.	66.4	gauche	SAZCIF	−8.4	eclipsed		
CIZWOX	37.0	staggered	41.4	gauche		−8.4	eclipsed	95.0	cis, C−H
CUJVOS	−78.2	stag. perp.	−32.0	gauche	SAZHEG	58.8	staggered	65.3	gauche
	−9.0	eclipsed	159.8	trans	SPPHOS	−9.8	eclipsed		
	−65.6	stag. perp.	−58.4	gauche		−79.7	stag. perp.		
CUJVUY	40.2	staggered	−140.3	cis, C−H	TEKKEZ	68.6	stag. perp.	66.3	gauche
	74.6	stag. perp.	−92.9	cis, C−H		70.0	stag. perp.	−156.8	trans
	−87.4	stag. perp.	−28.6	cis, C−C		−6.4	eclipsed	72.8	gauche
	−2.8	eclipsed	34.9	gauche	VEHREF	−20.9	staggered		
DESKOB	−63.2	stag. perp.	−55.5	gauche	VICFOC	−2.8	eclipsed		
	−2.9	eclipsed	79.4	gauche		1.0	eclipsed		
DEZLOJ	−10.0	eclipsed	−126.0	cis, C−H	VUKCEJ	61.2	stag. perp.	−122.2	cis, C−H
DINWIG	68.0	stag. perp.				−81.7	stag. perp.	−151.0	trans
EABTIZ	73.5	stag. perp.	179.5	trans		−54.5	staggered	139.3	cis, C−H
EMERIC	71.8	stag. perp.	−76.3	gauche		52.0	staggered		
FAMHEG	2.4	eclipsed	85.2	gauche	WIDGIZ	86.0	stag. perp.		
	−69.4	stag. perp.	−31.2	gauche	WISFOT	−86.9	stag. perp.	−67.0	gauche
FUPLAD	75.9	stag. perp.	76.9	gauche		−35.4	staggered	−59.2	gauche
	30.5	staggered	66.3	gauche		39.7	staggered	−174.6	trans
GAKNAH	52.7	staggered	173.4	trans	YALTEK	−4.2	eclipsed	−117.7	cis, C−H
GASJOZ	72.0	stag. perp.				67.4	stag. perp.	−157.5	trans
HYCANM	72.0	stag. perp.	46.3	gauche	YELGUR	59.5	staggered	29.4	cis, C−C
JUGPAC	−13.8	eclipsed	72.5	gauche	YUNYOV	−80.8	stag. perp.		
	−82.4	stag. perp.	160.4	trans	YUNYOV0	72.8	stag. perp.		
JUWZAC	45.6	staggered			YUNYUB	61.3	stag. perp.	22.6	cis, C−C
KAWTOR	22.0	staggered	66.4	gauche		73.7	stag. perp.	40.5	gauche
KEDKOT	−26.4	staggered			YUNZAI	−57.6	staggered	−19.9	cis, C−C
KOFJEU	−85.5	stag. perp.			ZENVAP	59.4	staggered		
KOHJIA	12.7	eclipsed	113.0	cis, C−H		46.5	staggered		
LIGYUW	−86.0	stag. perp.				46.0	staggered		
MDSPBF	23.0	staggered				46.3	staggered		
	−67.6	stag. perp.			ZOXLAZ	4.6	eclipsed	−67.6	gauche
MMXDPA	−19.3	staggered							
NADGEE	12.4	eclipsed							
	0.0	eclipsed							

[a] All dihedral angles in degrees. [b] C−C type determined by absolute value of the dihedral angle ∠(O−C−C−C): 0°−15° is eclipsed, 15°−60° is staggered, and 60°−90° is staggered perpendicular. [c] O−C type determined by absolute value of the dihedral angle ∠(H−O−C−C): 0°−30° is cis, CC 30°−90° is gauche, 90°−150° is cis, C−H 150°−180° is trans.

reported while others have not be determined.) In the remaining columns, we classify the structures according to the types **I**−**III**. We employ the following operational definitions for this classification. For the C−C type: 0°−15° is "eclipsed," 15°−60° is "staggered," and 60°−90° is "staggered perpendicular." And for the O−C type: 0°−30° is "cis, CC" or synperiplanar, 30°−90° is "gauche" or synclinal, 90°−150° is "cis, CH" or anticlinal, and 150°−180° is "trans" or antiperiplanar. These values were selected such that the limits coincide with the averages between adjacent types, and they are in accord with the IUPAC convention for conformation suggested by Klyne and Prelog.[22] Several of the structures contain either several symmetry-independent molecules or several $-CH_2OH$ groups within the same molecules or both, and each line entry characterizes one of these hydroxymethyl functions.

With regard to the conformation about the CC bond, all three types of structures occur, and there is no strong preference for any one of these (Table 2). Note in particular that more than a third of the structures fall into the category CC-eclipsed. The only structure type for which there exists no prototype to date is the all-eclipsed structure in which the hydroxyl HO-bond would be eclipsed with the CC bond, and this is very much understandable for steric reasons. Single-eclipsing either with regard to the CC bond or the CO bond is manifested in at least one structure. There is a preference for CO-staggered and CC-staggered perpendicular structures, and among these the gauche structures are some-

Table 2. Benzyl Alcohol Conformations in the Solid State Structures

		CO-type			
		staggered		eclipsed	
CC-type	total	trans antiperi-planar	gauche synclinal	cis, C−H anticlinal	cis, C−C synperi-planar
staggered	25	4	5	3	2
stag. perp.	35	8	13	2	2
eclipsed	23	1	7	5	0

(22) (a) See ref 10, p 21. (b) Klyne, W.; Prelog, V. *Experientia* **1960**, *16*, 521.

Table 3. Total Energies and Results of the Vibrational Analysis[a,b]

	molecule		RHF/6-31G*					MP2(full)
	C−C bond	C−O bond	energy	NI	VZPE	TE	*S*	energy
1a	staggered	s-trans	−344.584 451	0	89.80	94.02	83.40	−345.685 703
1b	staggered	s-gauche	−344.586 953	0	90.08	94.19	81.65	−345.688 464
1c	staggered	s-gauche	−344.582 887	1	89.76	93.47	77.90	−345.684 413
	staggered	s-cis		1		turns into **3d**		
2a	stag. perp.	s-trans	−344.583 412	1	89.84	93.50	77.60	−345.684 982
2b	stag. perp.	s-cis	−344.583 706	1	89.59	93.54	81.85	−345.685 265
2c	stag. perp.	s-gauche		0?		turns into **1b**		
3a	eclipsed	s-trans	−344.584 395	1	89.71	93.40	77.72	−345.685 358
3b	eclipsed	s-cis (CC)	−344.578 423	2	89.44	92.85	76.11	−345.679 611
3c	eclipsed	s-gauche		1?		turns into **1c**		
3d	eclipsed	s-cis (CH)	−344.583 333	1	89.47	93.40	80.99	−345.684 403
MeOH		staggered	−115.035 418	0	34.73	36.77	56.56	−115.353 295
MeOH		eclipsed	−115.033 252	1	34.30	36.12	55.39	−115.350 925

[a] All calculations employed the 6-31G* basis set. [b] Total energies in atomic units. Vibrational zero-point energies (VZPE) and thermal energies (TE) in kilocalories per mole und reported unscaled. Entropies (*S*) in calories per mole and per Kelvin.

what favored. Among the CC-staggered and CO-gauche structures, each structure shows the same sign of these two dihedral angles. (Whether the common sign is negative or positive determines absolute configuration of the molecule in the crystal. For the present discussion only relative stereochemistry matters.) One might expect that each CC-staggered conformation may realize both a +synclinal and a −synclinal CO-conformation. Because of the correlation between the CC- and OC-staggering, one of the synclinal CO-conformation is absent and only two of three a priori possible CO-staggered structures are realized. Among the CC-staggered perpendicular and CO-gauche structures, most have the same sign of the dihedral angles but there are a few structures that have dihedral angles of opposite sign. For the CC-staggered perpendicular structures, all three types of CO-staggering occur in the solid state.

Ab Initio Potential Energy Surface Analysis. Structures were optimized either without any symmetry constraints, C_1, or with the geometry constrained to C_s symmetry.[23] The nature of any stationary structure optimized in C_s symmetry was evaluated by way of vibrational analyses; such structures were identified as minima, transition-state structure, or second-order saddle point structures, respectively, by the presence of zero, one, or two imaginary vibrational frequencies, respectively.[24] The structures of chiral transition-state structures were located using gradient algorithms for the location of saddle points on the potential energy hypersurface. The searches for stationary structures in most cases were conducted starting with a force constant matrix computed for the initial trial structure. For all stationary structures, accurate second derivatives of the energy were computed to acertain that a stationary structure had indeed been located and to obtain vibrational zero-point energies.

The π-density of the phenyl group presents a polarizable medium[25] and may be sensitive to induced polarization. The C−O and the O−H bonds both are highly polar and intramolecular polarization may be an important mechanism of electronic relaxation and stabilization. Hence, we carried out all optimizations not only at the restricted Hartree−Fock level, RHF, but also at the correlated level using second-order Møller−Plesset perturbation theory, MP2(full).[26] The split-valence and polarization function augmented basis set 6-31G* was employed in all cases. The vibrational frequencies were determined analytically.

The ab initio quantum-mechanical calculations were carried out with the program Gaussian 94[27] on a Silicon Graphics PowerChallenge L minisupercomputer with 8 R10000 processors. Pertinent results are summarized in Table 3. We report the total energies computed at the theoretical levels RHF/6-31G* and MP2(full)/6-31G*, and we report results of the vibrational analysis performed at the RHF/6-31G* level.

A natural population analysis[28] (NPA) was carried out at the MP2(full)/6-31G* level of theory to determine atomic charges.

Results and Discussion

Stationary Structures with CC-Staggered Conformations. For methanol, H_3COH, the conformational issue is simple. The rotational energy profile presents a 3-fold barrier where the staggered and eclipsed structures, respectively, are minima and transition-state structures for rotation. The rotational barrier in methanol has been studied in detail, and the origin of the rotational barrier remains a matter of debate.[29] The replacement of one H-atom by a phenyl group complicates matters considerably. Not only does the presence of the phenyl group in $PhCH_2OH$ remove degeneracies, but it

(23) For an excellent introduction to potential energy surface analysis, see: *Theoretical Aspects of Physical Organic Chemistry*; Shaik, S., Schlegel, H. B., Wolfe, S., Eds.; John Wiley & Sons: New York, NY, 1992; Chaper 2.

(24) Stanton, R. E.; McIver, J. W., Jr. *J. Am. Chem. Soc.* **1975**, *97*, 3632.

(25) For recent articles on the dipole polarizability of benzene, see: (a) Millefiori, S.; Alparone, A. *THEOCHEM* **1998**, *422*, 179. (b) Hinchliffe, A.; Soscun, M. H. J. *Asian J. Spectrosc.* **1997**, *1*, 77.

(26) (a) Hehre, W. J.; Radom, L.; Schleyer, P. v. R.; Pople, J. A. *Ab Initio Molecular Orbital Theory*; John Wiley & Sons: New York, NY, 1986. (b) Leach, A. R. *Molecular Modelling*; Addison-Wesley Longman Limited: Essex, England, 1996.

(27) Frisch, M. J.; Trucks, G. W.; Schlegel, H. B.; Gill, P. M. W.; Johnson, B. G.; Robb, M. A.; Cheeseman, J. R.; Keith, T.; Petersson, G. A.; Montgomery, J. A.; Raghavachari, K.; Al-Laham, M. A.; Zakrzewski, V. G.; Ortiz, J. V.; Foresman, J. B.; Cioslowski, J.; Stefanov, B. B.; Nanayakkara, A.; Challacombe, M.; Peng, C. Y.; Ayala, P. Y.; Chen, W.; Wong, M. W.; Andres, J. L.; Replogle, E. S.; Gomperts, R.; Martin, R. L.; Fox, D. J.; Binkley, J. S.; Defrees, D. J.; Baker, J.; Stewart, J. P.; Head-Gordon, M.; Gonzalez, C.; Pople, J. A. Gaussian 94, revision C.3; Gaussian, Inc.: Pittsburgh, PA, 1995.

(28) (a) Glendening, E. D.; Reed, A. E.; Carpenter, J. E.; Weinhold, F. *NBO Ver. 3.1*. (b) Glendening, E. D.; Weinhold, F. *J. Comput. Chem.* **1998**, *19*, 628, and references therein.

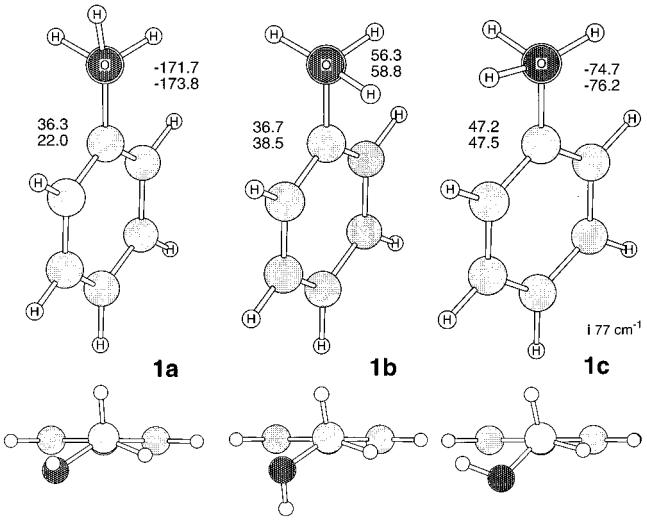

Figure 1. Molecular models of stationary structures of CC-staggered benzyl alcohol. The MP2(full)/6-31G* structures are shown. Values of the ∠(O−C−C−C) and ∠(H−O−C−C) dihedral angles are given on left and right, respectively, as determined at the theoretical levels MP2(full)/6-31G* and RHF/6-31G*. For the transition state **1c**, the imaginary frequency associated with the transition vector is given as determined at the level RHF/6-31G*.

affects the character of the various CO-conformations on the potential energy hypersurface.

Newman projections are shown in Figure 1 of the stationary structures with CC-staggered conformations of type **I**. We first considered benzyl alcohol in which the dihedral angle ∠(H−O−C−C) was close to 180° or CO-s-trans, and the exo structure **1a** was found to be a minimum. A second and slightly more stable endo minimum, **1b**, was located in which the dihedral angle ∠(H−O−C−C) was close to 60° or CO-s-gauche. Both of these structures **1a** and **1b** are CC-staggered with ∠(H−O−C−C) dihedral angles of close to 36°. This value is significantly lower than the value of 54° suggested by the electron diffraction study.[16] Note that deformations about the CC bond require little energy (vide infra), and the electron diffraction study returns time-averaged structure information. The third staggered structure shown, **1c**, is interesting for several reasons. To begin with, note that **1b** and **1c** are not enantiomers but diastereoisomers as the result of the orientation of the phenyl group. More interesting is the fact that **1c** is a transition-state structure and not a minimum. The structure **1c** is a transition-state structure for the conversion of **1a** into **1b** by way of "counterclockwise" rotation about the CO bond (of the enantiomers drawn in Figure 1) and vice versa. We also searched for a transition-state structure for the isomerization of **1a** into **1b** by way of clockwise rotation about the CO bond. Yet, attempts to locate a transition-state structure of type **1d** in which the OH bond was eclipsed with one of the CH bonds (Scheme 2) were not successful; all these attempts resulted in structure **1c**. We will return to this issue in the discussion of structure **3d**.

Scheme 2. Trial Structure 1d Used in the Search for a Transition State. These Searches Resulted in the Stationary Structure 1c

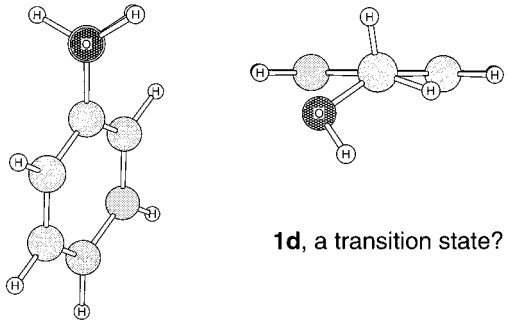

Stationary Structures with CC-Staggered Perpendicular Conformations. Structures **2a** and **2b** were optimized in C_s symmetry (Figure 2), and the vibrational analysis revealed these structures to be transition-state structures. Note that Bernstein et al.[17] tentatively had assigned this structure **2b** to the only conformer detected in their MRES study. The transition-state vector of **2a** clearly shows a rotation around the C−C bond and leaves no doubt that **2a** is the transition-state structure for the enantiomerization of **1a**. Note that the frequency of the imaginary mode is very low, and it demonstrates that the potential energy hypersurface is quite shallow in the region along the path of enantiomerization of **1a**. The

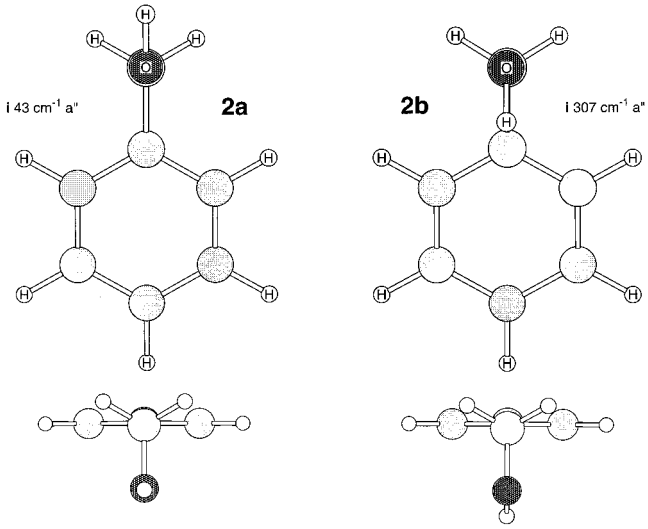

Figure 2. Molecular models of stationary structures of CC-staggered perpendicular benzyl alcohol. The MP2(full)/6-31G* structures are shown. The imaginary frequencies associated with the transition vectors are given as determined at the level RHF/6-31G*.

transition-state vector for **2a** is very much different. In this case, the imaginary mode a″ is significantly higher in magnitude and the transition-state vector indicates a displacement of the H atom akin to moving the H atom between enantiomeric gauche positions. For **2a**, it is the first real vibration (34 cm^{-1}, a″) whose normal mode corresponds to a rotation about the C−C bond. Thus, it seemed that there might exist a minimum structure of type **II** with CO-s-gauche conformation, **2c**. Our data mining revealed several benzyl alcohol derivatives that realize such structures in the solid state. Table 1 contains 13 entries of the type CC-staggered perpendicular and

(29) (a) Badenhoop, J. K.; Weinhold, F. *Int. J. Quantum Chem.* **1999**, *72*, 269. (b) Pophristic, V.; Goodman, L.; Guchhait, N. *J. Phys. Chem. A* **1997**, *101*, 4290. (c) Chung-Phillips, A.; Jebber, K. A. *J. Chem. Phys.* **1995**, *102*, 7080. (d) Knight, E. T.; Allen, L. C. *J. Am. Chem. Soc.* **1995**, *117*, 4401. (e) Wu, Yun Dong; Houk, K. N. *J. Phys. Chem.* **1990**, *94*, 4856.

Chart 1

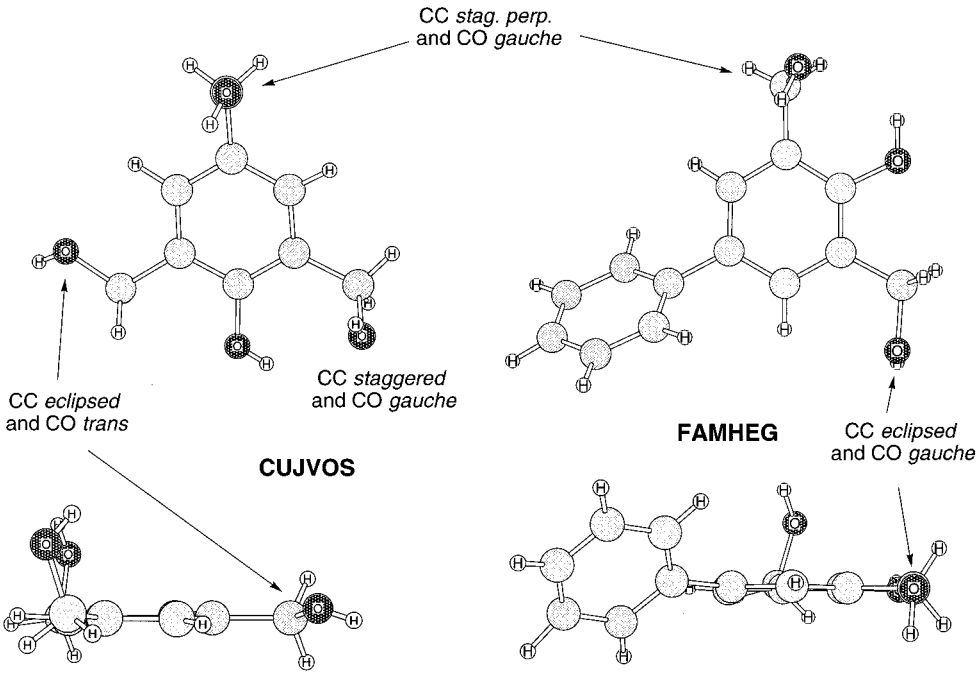

CO-s-gauche, and in Chart 1 we show two compelling examples. The CSD database entries CUJVOS (2,4,6-tris(hydroxymethyl)phenol[30]) and FAMHEG (2,6-bis(hydroxymethyl)-4-phenylphenol[31]) both contain a hydroxymethyl group that is oriented almost perfectly perpendicular with respect to the benzene ring and with the staggered hydroxyl H atom pointing inward. We have searched for such a structure beginning with an appropriate trial structure (Scheme 3) and with a computed

Scheme 3. Trial Structure 2c Used in the Search for a Potential Minimum. These Searches Resulted in the Stationary Structure 1b

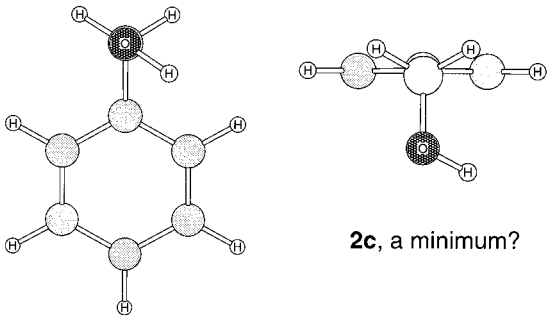

Hessian matrix. Yet, no such structure could be located, and instead, all of these attempts resulted in the minimum **1b**. As the H atom in **2b** is displaced out of the molecular symmetry plane in one direction, the O atom begins to rotate around the CC bond in the opposite direction. In other words, as **1b** progresses toward **2b** the hydroxyl H atom first moves through the plane that becomes the symmetry plane of **2b** and then returns to that plane when the CO-s-gauche conformations turns CO-s-cis in the late stage of the **1b** to **2b** distortion.

Stationary Structures with CC-Eclipsed Conformations. The entries in Tables 1 and 2 show that many benzyl alcohols crystallize with CC *eclipsed* conformations in which the OC conformation may be either trans or gauche. Chart 1 provides examples of both of these situations. A C_s-symmetric structure of type **III** and CO-s-trans was optimized, and this structure **3a** was found to be a transition-state structure. The recent study by Ebata et al.[18] suggested that **3a** is the structure of the less stable minimum observed in their jet studies. We believe the Ebata result to be an artifact caused by the use of the unpolarized 6-31G basis set. The early RHF/STO-3G results[13] also show that insufficient basis sets artifically favor **3a**. The transition-state vector clearly indicates a displacement corresponding to a rotation about the CC bond, and the frequency of the imaginary mode shows the potential energy surface in that region to be exceedingly flat. Hence, structure **3a** serves as the transition-state structure for the enantiomerization of **1a**. The other C_s-symmetric structure **3b** corresponds to a second-order saddle point on the potential energy hypersurface. The displacement vector of the imaginary mode with the higher absolute frequency shows an H-atom rotation about the CO bond. The displacement vector of the other imaginary mode indicates a rotation about the CC bond. The analysis of the imaginary normal modes

Scheme 4. Trial Structure 3c Used in the Search for a Potential Transition-State Structure. This Search Resulted in the New Transition-State Structure 3d

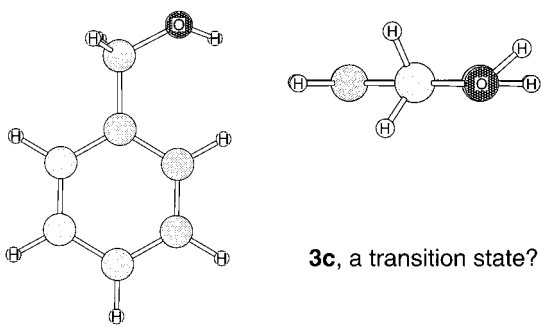

(30) Perrin, M.; Perrin, R.; Thozet, A.; Hanton, D. *Polymer Prepr.* **1983**, *24*, 163.
(31) Perrin, M.; Cherared, M. *Acta Crystallogr., Sect. C* **1986**, *42*, 1623.

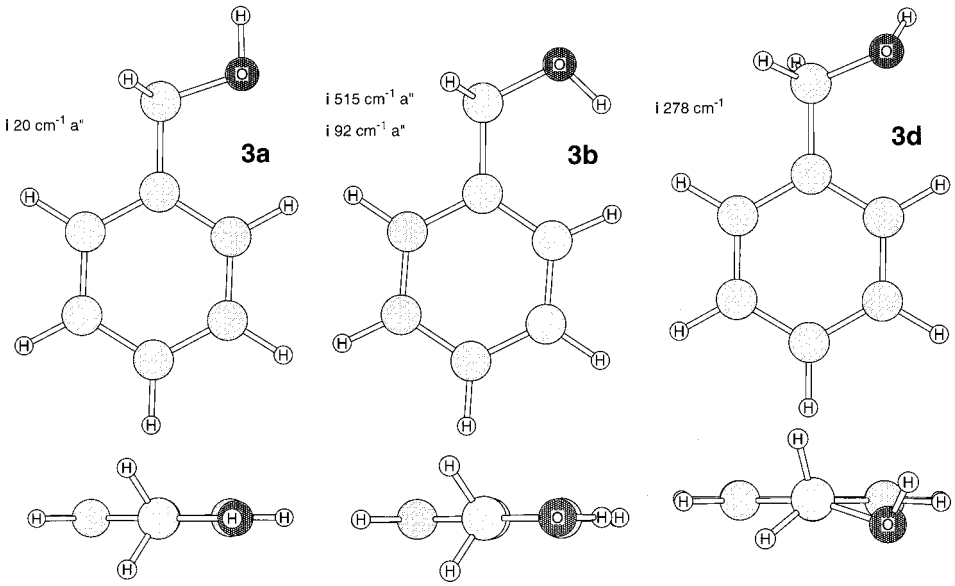

Figure 3. Molecular models of stationary structures of CC-eclipsed benzyl alcohol. The MP2(full)/6-31G* structures are shown. The imaginary frequencies associated with the transition vectors are given as determined at the level RHF/6-31G*.

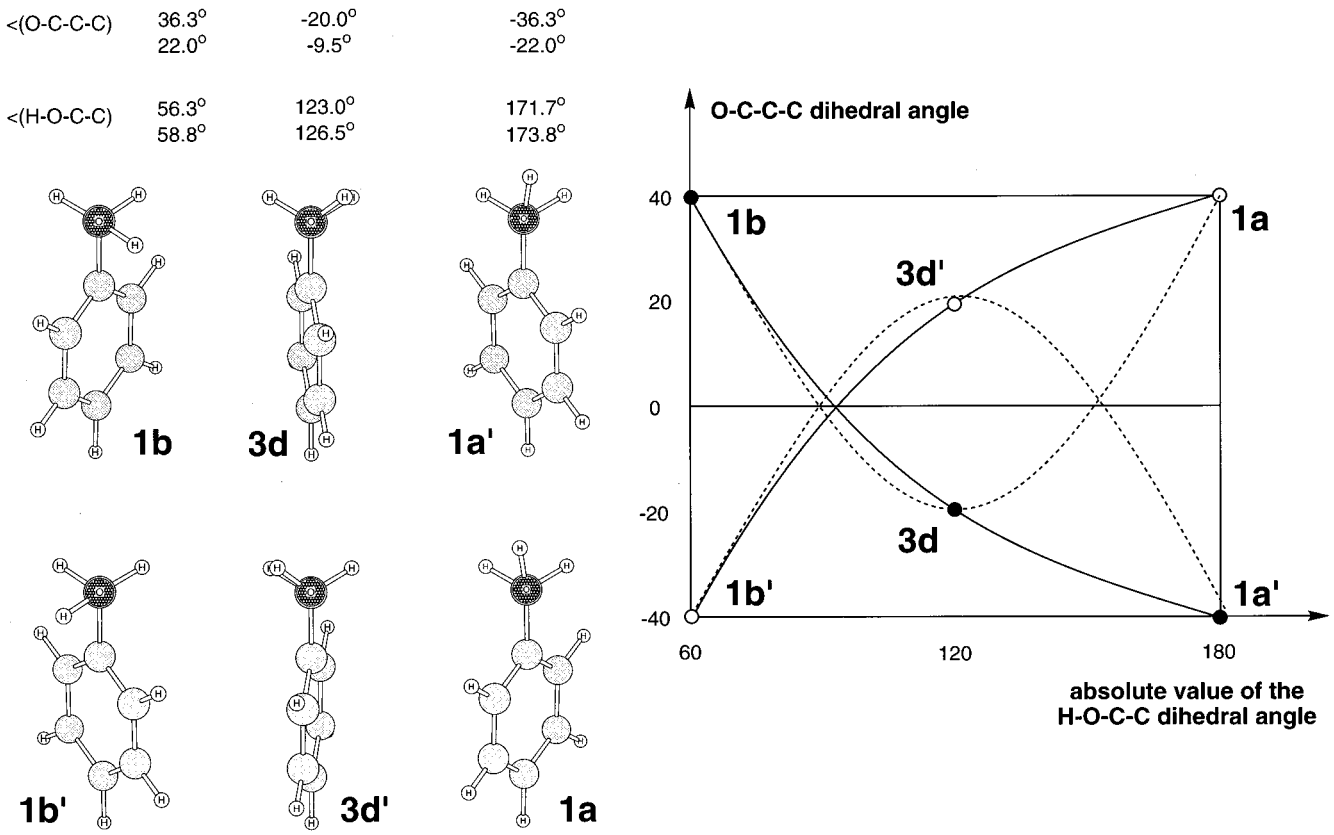

Figure 4. Diastereomerization of **1a** and **1b**. Continuous change in both the ∠(H−O−C−C) and the ∠(O−C−C−C) dihedral angles afford the diastereomerization of enantiomer **1b** in **1a′**. The values apply to the top row of structures, and they are the ∠(H−O−C−C) and the ∠(O−C−C−C) dihedral angles determined at the theoretical levels MP2(full)/6-31G* and RHF/6-31G*. The enantiomerically related diastereomerization path is shown on the bottom.

suggested that there might exist a second transition-state structure of type **III**, one with a CO-s-gauche conformation. We suspected that structure to be staggered with regard to the CO bond and employed an initial trial structure of type **3c** (Scheme 4). Starting with structure **3c** and searching for a transition-state structure did, however, result in the transition-state structure **3d** shown in Figure 3. This structure **3d** is no longer eclipsed with regard to the CC bond, while it has turned eclipsed with regard to the CO bond! The transition vector of **3d** is dominated by an H-rotation about the CO bond. Yet, such a rotation about the CO bond cannot be the only process going on along this reaction path simply because there are no minima that could be interconverted in this

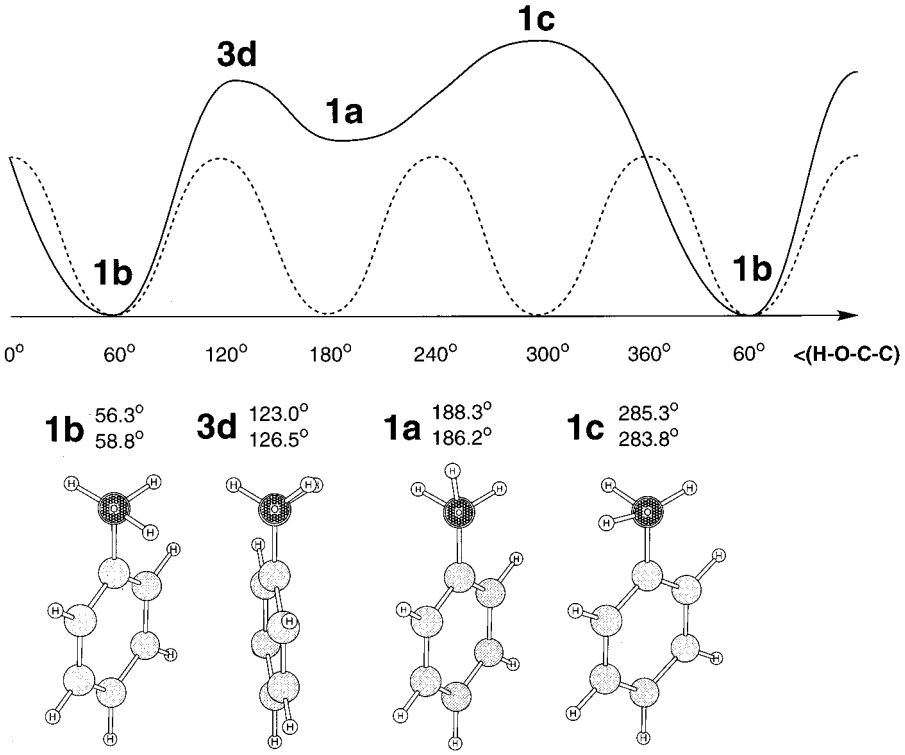

Figure 5. Schematic but to scale rendition of the rotational energy profile about the CO bond of benzyl alcohol. The dashed line represents the rotational energy profile of methanol. Molecular models of the MP2(full)/6-31G* structures are shown. Values of selected structural parameters as determined at the theoretical level MP2(full)/6-31G*.

way. An inspection of the normal mode with the lowest real frequency clarifies the situation in an interesting manner. The real mode corresponds to rotation about the CC bond, and it has a rather low frequency. Much like in the case of the path connecting **1b** and **2b** discussed above, the displacement vector associated with the imaginary mode reflects only one component of a reaction coordinate for isomerization that requires more than one internal coordinate for a complete description. In this case, structure **3d** is the transition-state structure for the diastereomerization of structures **1a** and **1b**! Structure **3d** fills the gap that was left by the unsuccessful search for **1d** (vide supra). Note that **1d** and **3d** differ in the direction of the phenyl twist, and this explains the difficulty in locating this structure initially.

The process of diastereomerization between **1a** and **1b** is illustrated in Figure 4. The process is one that involves the stereospecific isomerization of one enantiomer of **1a** into one enantiomer of **1b**. If the structures shown in Figures 1 and 3 are one set of enantiomers, we refer to their mirror images by adding a prime as a superscript. Enantiomer **1b** will be converted into **1a′** rather than **1a**. Intramolecular motions prefer "direct" trajectories to maintain momentum, that is, they prefer to be steady (solid lines to the right of Figure 4) rather that to revert halfway through the process (dashed lines).[32] The diastereomerization of **1b** to **1a** or of **1b** to **1a′** both entail a steady increase in dihedral angle ∠(H−O−C−C). However, the former process would start out with a rotation about the CC bond in one direction and then rotate about that bond in the opposite direction in the second half of the isomerization path. The latter process, on the other hand, involves a rotation about the CC bond in the same direction along the entire diastereomerization path and this is the process that actually occurs.

Rotational Energy Profiles. A schematic rotational energy profile associated with the rotation about the C−O bond is shown in Figure 5. The horizontal axis shows the dihedral angle ∠(H−O−C−C), and the vertical axis indicates relative energy. Relative energies determined at the MP2(full)/6-31G* level are given. The dashed line shows the rotational energy profile of methanol, that is, a profile with a 3-fold barrier where the staggered structures are minima and the eclipsed structures are the transition-state structures for rotation. Figure 5 illustrates in a compelling fashion the dramatic effects of the replacement of one H by a phenyl group! The H/Ph replacement necessarily removes the 3-fold degeneracy of the minimum and one might have expected either a situation in which there are two different staggered structures to consider or a situation with three different staggered structures if the phenyl plane is oriented in a way that precludes two C−O staggered structures to become a pair of enantiomers. Yet, the actually realized scenario entails only two minimum structures, **1a** and **1b**, and the third staggered structure, **1c**, turns out to be a transition state structure.

The rotational energy profiles for the enantiomerizations of **1a** and **1b** are depicted in Figure 6. The vertical scale is the same as the one used in Figure 5. The enantiomerization of **1a** is a very facile process, less than 0.5 kcal/mol, no matter whether the process involves a motion of the hydroxyl group through the plane of the benzene via **3a** or a swinging between the enantiomeric minima on the same face of the benzene via **2a**. The enantiomerization of **1b** also is a facile process so long

(32) Carpenter, B. *Angew. Chem., Int. Ed. Engl.* **1998**, *37*, 3340, and references cited therein.

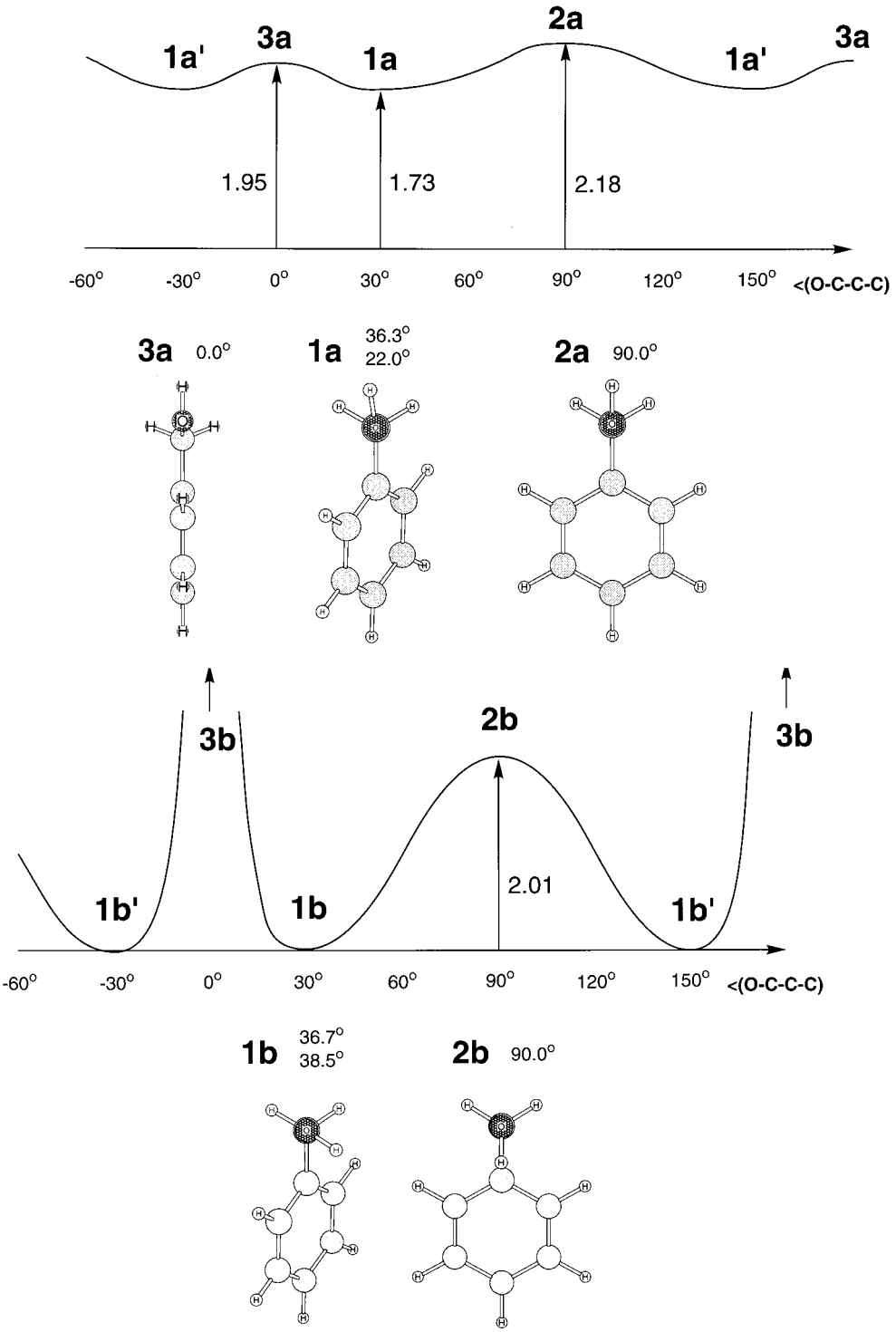

Figure 6. Enantiomerization profiles of **1a** and **1b**.

as the hydroxyl group ramains on the same face of the benzene ring. A direct enantiomerization of **1b** with a motion of the hydroxyl group through the plane of the benzene can be avoided by a sequence involving diastereomerization (**1b** to **1a**′), enantiomerization (**1a**′ to **1a**), and again diastereomerization (**1a** to **1b**′).

Thermochemistry. So far, we have discussed relative energies between stationary structures. The relative energies, E_{rel}, are computed as the difference between the total energies. We have determined relative energies based on the total energies computed at the levels RHF/6-31G* and MP2(full)/6-31G*, and these are listed in Table 4. There are only very small differences between these sets of data, and we have discussed the E_{rel} values determined at the MP2(full)/6-31G* level. The relative energies do not account for any enthalpy and entropy effects associated with thermal motion, and several improvements can be made. At absolute zero, the motion shows up only in the vibrational zero-point energy while rotation and translations are frozen. The consideration of the differences ΔVZPE between the zero-point vibrational energies VZPE then yields relative enthalpies, $H'_{rel} = E_{rel} + \Delta VZPE$. The next level of sophistication considers the thermal energies TE computed for room temper-

Table 4. Relative Stabilities[a-c]

	molecule		RHF					MP2(full)			
	C−C bond	C−O bond	E_{rel}	ΔVPE	ΔTE	$-T\Delta S$	ΔG	E_{rel}	H'_{rel}	H_{rel}	G_{rel}
1a	staggered	s-trans	1.57	−0.28	−0.17	−0.52	−0.69	1.73	1.45	1.56	1.04
1b	staggered	s-gauche	0.00	0.00	0.00	0.00	0.00	0.00	0.00	0.00	0.00
1c	staggered	s-gauche	2.55	−0.32	−0.72	1.12	0.40	2.54	2.22	1.82	2.94
2a	stag. perp.	s-trans	2.22	−0.24	−0.69	1.21	0.52	2.18	1.94	1.49	2.70
2b	stag. perp.	s-cis	2.04	−0.49	−0.65	−0.06	−0.71	2.01	1.52	1.36	1.30
3a	eclipsed	s-trans	1.61	−0.37	−0.79	1.17	0.38	1.95	1.58	1.16	2.33
3b	eclipsed	s-cis (CC)	5.35	−0.64	−1.34	1.65	0.31	5.56	4.92	4.22	5.87
3d	eclipsed	s-cis (CH)	2.27	−0.61	−0.79	0.20	−0.59	2.55	1.94	1.76	1.95
MeOH		staggered	0.00	0.00	0.00	0.00	0.00	0.00	0.00	0.00	0.00
MeOH		eclipsed	1.36	−0.43	−0.65	0.35	−0.30	1.49	1.06	0.84	1.19

[a] All calculations employed the 6-31G* basis set. [b] Changes in the vibrational zero-point energies (VZPE), thermal energies (TE), temperature weighted entropies ($T\Delta S$) all are in kilocalories per mole und unscaled. [c] $H'_{rel} = E_{rel} + \Delta$VZPE; $H_{rel} = E_{rel} + \Delta$TE; and $G_{rel} = E_{rel} + \Delta G$.

ature and including vibrational, rotational, and translation energies. The consideration of the differences ΔTE between the thermal energies yields the relative enthalpies, $H_{rel} = E_{rel} + \Delta$TE. The equilibria between stationary structures at constant pressure and temperature are determined by their relative free enthalpies, G_{rel}. The G_{rel} values are determined by augmentation of the relative energies by $\Delta G = \Delta$TE $- T\Delta S$. In Table 4, we have listed the contributions ΔVZPE, ΔTE, $T\Delta S$, and ΔG determined at the RHF/6-31G* level and the values of H'_{rel}, H_{rel}, and G_{rel} that are based on the relative energies computed at the MP2(full)/6-31G* level. Note that we have not applied any scaling to the thermal energies. Vibrational frequencies are overestimated by about 10%, and they require scaling. Differences between vibrational zero-point energies or thermal energies, however, are hardly affected by the scaling.

The consideration of the thermochemistry leads to excellent agreement between experiment and theory. While relative energies indicate a preference of close to 2 kcal/mol for the endo structure, the relative free enthalpy preference is 1.04 kcal/mol and in excellent agreement with NMR data.[14] Furthermore, the data collected in Table 4 show that all pertinent relative energies and relative free enthalpies are less than 3 kcal/mol. Benzyl alcohol, therefore, is a highly flexible molecule that allows for essentially unhindered enantiomerization and diastereomerization of the two minima.

The low-energy requirements for conformational distortion of benzyl alcohol allow for the optimization of intermolecular interactions in the crystals. Hence, the conformational map (Figure 7) shows utter scatter and demonstrates in a compelling fashion that no deductions about instrinsic conformational preference can be made on the basis of solid-state data.

Origin of the C−O Conformational Preferences. The stability of the endo structure **1b** had been attributed to intramolecular OH···π-density hydrogen bonding.[33] Alternatively, it has been argued that the exo structure **1a** is disadvantaged because of the electron−electron repulsion between the O-lone pairs and the benzene π-cloud and that there is no evidence for OH···π-density hydrogen bonding.[14,34] We propose an explanation of the relative stabilities of **1a**−**c** that considers the conformation dependences of the effects of electron−electron repulsion between the O lone pairs and the benzene π-cloud, the charge−charge attraction between the hydroxyl H atom and the benzene π-density, and the dipole−dipole interaction associated with the CH_2-C_{ipso} and −OH bonds. Note that the charge−charge attraction between the hydroxyl H atom and the benzene π-density would be very much different from the OH···π-density hydrogen bonding invoked by others. Hydrogen bonding is a special case of dipole−dipole interaction and requires a permanent dipole of the H-bond acceptor. We carried out electronic structure analyses of various benzyl alcohols to test and to distinguish between the hypotheses concerning the interaction between the hydroxyl group and the phenyl ring. The relative energies between the various stationary structures are small and any explana-

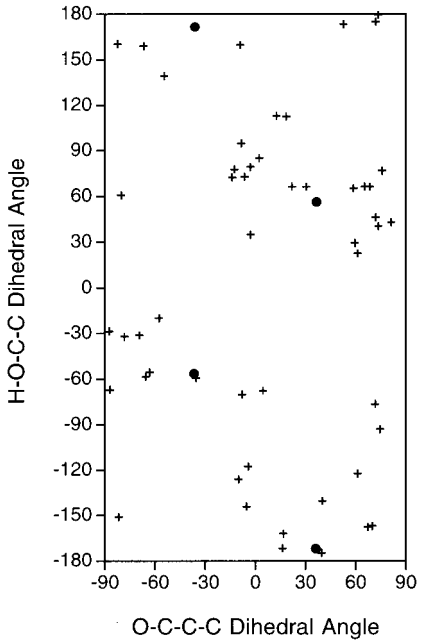

Figure 7. Conformational map of benzyl alcohol. The "+" marks refer to the solid-state structures collected in Table 1, and the "●" mark the structures of the enantiomeric pairs of the computed minima.

(33) (a) Schleyer, P v. R.; Trifan, D. S.; Baeskai, R. *J. Am. Chem. Soc.* **1958**, *80*, 6691. (b) Luck, W. A. P. In *The Hydrogen Bond*; Schuster, P., Zundel, G., Sandorfy, C., Eds.; North-Holland: Amsterdam, The Netherlands, 1976; Vol. 2, Chapter 11.

(34) (a) Bakke, J. M.; Ronneberg, H.; Chadwick, D. J. *J. Magn. Reson. Chem.* **1987**, *25*, 251. (b) Abraham, R. J.; Bakke, J. M.; Skjetne, T. *Acta Chem. Scand. Ser. B* **1984**, *B38*, 547. (c) Abraham, R. J.; Bakke, J. M. *Acta Chem. Scand. Ser. B* **1983**, *B37*, 865. (d) Abraham, R. J.; Bakke, J. M. *Acta Chem. Scand. Ser. B* **1981**, *B35*, 367.

Table 5. Atomic Charges in Various Conformations of Benzyl Alcohol[a]

atom or group	**1a**	**1b**	**1c**	**2a**	**2b**
H(O)	0.479	0.476	0.474	0.473	0.480
O	−0.756	−0.752	−0.748	−0.752	−0.756
$C(CH_2)$	−0.099	−0.102	−0.103	−0.103	−0.104
$H(CH_2)$	0.201	0.232	0.207	0.200	0.212
$H(CH_2)$	0.206	0.200	0.224	0.200	0.212
C_{ipso}	−0.071	−0.091	−0.075	−0.071	−0.100
C_{ortho}	−0.220	−0.229	−0.225	−0.215	−0.224
$C_{ortho'}$	−0.230	−0.229	−0.225	−0.215	−0.224
C_{meta}	−0.230	−0.229	−0.229	−0.232	−0.229
$C_{meta'}$	−0.232	−0.230	−0.230	−0.232	−0.229
C_{para}	−0.236	−0.234	−0.233	−0.231	−0.230
$H(C_{ortho})$	0.250	0.248	0.222	0.235	0.239
$H(C_{ortho'})$	0.231	0.233	0.233	0.235	0.239
$H(C_{meta})$	0.235	0.236	0.236	0.236	0.239
$H(C_{meta'})$	0.235	0.236	0.237	0.236	0.239
$H(C_{para})$	0.235	0.236	0.236	0.235	0.239
Σ	−0.002	0.001	0.001	−0.001	0.003
$q(C_i) + q(C_o) + q(C_{o'})$	−0.521	−0.549	−0.525	−0.501	−0.548
$q(C_p) + q(C_m) + q(C_{m'})$	−0.698	−0.693	−0.692	−0.695	−0.688
CH_2	0.308	0.330	0.328	0.297	0.320
OH	−0.277	−0.276	−0.274	−0.279	−0.276
CH_2OH	0.031	0.054	0.054	0.018	0.044
$\Delta = q(CH_2) - q(C_{ipso})$	0.379	0.421	0.403	0.368	0.420
$\Pi = q(H) - q(O)$	1.235	1.228	1.222	1.225	1.236
ν(OH)[c]	3678	3658	3686	3662	3686

[a] All charges were determined on the basis of the MP2(full)/6-31G* electron densities. [b] For benzene at MP2(full)/6-31G*, $q(H) = +0.235$. [c] The HO stretching frequencies are given in cm^{-1} as computed at RHF/6-31G* and scaled by the usual factor of 0.8929.

tion of these small differences necessarily is of a qualitative nature since there is no rigorous way to quantitate all factors invoked to contribute to the stability ordering. However, the electron density analyses allow one to see whether an explanation is at least consistent with the electron density distribution and, thus, to distinguish among competing explanations.The results of natural population analyses at the MP2(full)/6-31G* level are summarized in Table 5. Interestingly, the atomic charges indicate hardly any long-range effects of the hydroxymethyl group on the benzene moiety. Benzene itself shows a charge separation of 0.235 for the C−H bond with the H atom being the positive pole. The charges for all of the aromatic H-atoms in **2a** and **2b** are essentially the same as in benzene. For **1a**−**c**, the charges of the H-atoms in the para position, both meta positions, and the distant ortho position ($H_{ortho'}$) also are essentially the same as in benzene and only the proximate *o*-H atom shows variations. The hydroxymethyl group overall is a slightly electron-withdrawing group with $0.018 < q(CH_2\text{-}OH) < 0.054$ and, considering that $q(H) = 0.235$ in benzene, it follows that the C_6H_5 fragment is being deprived by about 0.217−0.181 electrons upon hydroxymethyl substitution. These electrons come mostly from C_{ipso}, which shows negative charges in the range between −0.071 and −0.100, and the *o*-C atom charges also are slightly reduced as the consequence of polarization. The charge distribution in the overall nearly neutral hydroxymethyl group is highly quadrupolar: The H atom is positively charged (0.476 ± 0.004), the O atom is highly negatively charged (-0.753 ± 0.005), and the CH_2 group is very much positively charged (0.317 ± 0.013). In Table 5, we have also included the values for $\Delta = q(CH_2) - q(C_{ipso})$; this term provides a parameter for the polarity of the CH_2-C_{ipso} bond, and it shows an interesting variation with conformation. For **2b**, the Δ value assumes a maximum; this conformation benefits from an enhanced polarization of the CH_2-C_{ipso} bond since it maximizes the attraction associated with the dipole antiparallel alignment of the OH and CC bonds (Figure 8). On the other hand, the Δ value assumes a minimum for **2a**. In the conformation of **2a**, the dipole−dipole interaction is small—on the borderline between repulsion of side-by-side and attraction between head-to-tail parallel-aligned dipoles—and there is no benefit associated with a large polarization of the CH_2-C_{ipso} bond. Structures **1a** and **1b** show Δ values that are similar to those of **2a** and **2b** and for same reasons.

In Figure 8, the molecules **1a**−**c** are shown in a side view that allows one to see the alignment of the HO bond moment relative to the benzene π-cloud. The preference for **1b** becomes immediately understandable: This arrangement is good to begin with since the positively charged hydroxyl H atom is placed close to the π-density to allow for optimal charge−charge attraction, and the O lone pairs are placed to avoid electron−electron repulsion with the π-cloud. To improve matters even more, this conformation benefits greatly from the indicated polarization of the CH_2-C_{ipso} bond; the CH_2-C_{ipso} bond polarity favors dipole−dipole attraction with the OH bond and polarization enhances this attraction further. Structure **1a** is handicapped from the start due to electron−electron repulsion between the O-lone pairs and the π-cloud. Furthermore, structure **1a** benefits little from the dipole−dipole interaction between the CH_2-C_{ipso} and OH bonds. The structures **1b** and **1c** have ∠(H−O−C−C) angles with about equal magnitude and dipole−dipole interactions between the CH_2-C_{ipso} and OH bonds should be largely the same. It appears that the major disadvantage of **1c** lies with the placement of the hydroxyl H-atom in a position that does not allow for charge−charge attraction between the hydroxyl H-atom and the π-density.

At the end of Table 5, we have also included computed and scaled frequencies of the HO stretching modes. The magnitude of these vibrational frequencies have been used to make deductions about OH···π-density interactions.[18] Such deductions are not straightforward in light of the fact, that, for example, the computed HO stretching frequency of **2a** (OH away from π-density) is just about equal to the one computed for **1b** (OH close to π-density).

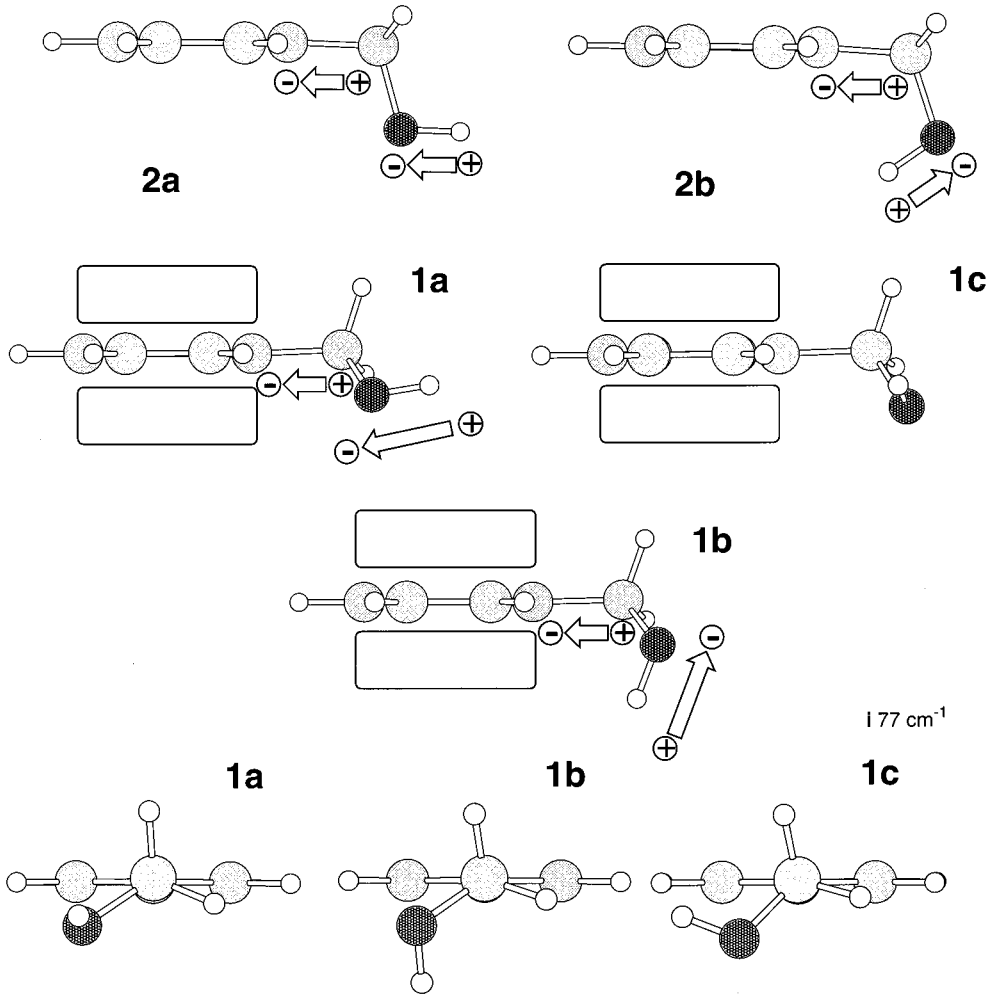

Figure 8. Side views of the MP2(full)/6-31G* structures of **1a**−**c** and **2a**,**b**. The dipole moment of the CH_2-C_{ipso} and the O−H bonds are indicated schematically by arrows. The rectangles drawn for **1** indicate the π-density regions above and beyond the plane of the benzene rings.

Moreover, there is no simple correlation between the HO bond polarity, as measured by the parameter $\Pi = q(H) - q(O)$, and the HO stretching frequency.

Conclusion

The existence of two minima of benzyl alcohol has been known from the spectroscopic evidence for some time, and the two minima were found to correspond to the exo and endo structures, with the latter being preferred. The structural discussions have focused from the start on whether the OH bond is either oriented away or toward the benzene ring. The former results in a CO-staggered conformation, while the latter could give a CO-eclipsed conformation if the best CC conformation is staggered perpendicular. Yet, the theoretical discussions of the conformational space of benzyl alcohol and the electron diffraction study in particular suggested early on that the endo structure is not staggered perpendicular but that it is staggered instead. If that is so, then there is of course no longer any reason to assume a CO-eclipsed conformation in the endo structure, and one wonders why there has never been any discussion of a potential third minimum, the third of the conformations that are CO-staggered. With a view to methanol, the consideration of a 3-fold barrier about the CO bond should have been the first consideration. The experiments show that such a third minimum would have to exist in low concentration, but they do not exclude such a local minimum. Our potential energy surface analysis now shows that there are in fact only two minima and that the third CO-staggered structure is a transition state structure.

Acknowledgment. We thank the Research Support Computing Group of Information Access and Technology Services Division of the University of Missouri for computer resources. G.R.N. was the recipient of a Howard Hughes Medical Institute Research Fellowship in AY1998-9 and during the summer of 1999. We thank Michael Lewis for the performance of the CSD searches.

Supporting Information Available: Pdb files of all stationary structures and a version of Table 1 in which the names of the CSD records serve as links to displaying the solid-state structures of the molecules. This material is available free of charge only via the Internet at http://pubs.acs.org.

JO991423Q